

Using Convolutional Neural Networks for fault analysis and alleviation in accelerator systems

Jashanpreet Singh Sraw

Thapar Institute of Engineering and Technology
Patiala, India

Deepak M C

PES College of Engineering
Mandya, India

Abstract—Today, Neural Networks are the basis of breakthroughs in virtually every technical domain. Their application to accelerators has recently resulted in better performance and efficiency in these systems. At the same time, the increasing hardware failures due to the latest (shrunked) semiconductor technology needs to be addressed. Since accelerator systems are often used to back time-critical applications such as self-driving cars or medical diagnosis applications, these hardware failures must be eliminated. Our research evaluates these failures from a systemic point of view. Based on our results, we find critical results for the system reliability enhancement and we further put forth an efficient method to avoid these failures with minimal hardware overhead.

Index Terms—fault analysis, neural networks, accelerator systems, deep neural networks

I. INTRODUCTION

Deep neural networks (DNNs) have been demonstrated to be successful in massive territories like image processing, video processing, and natural language processing over the years [1]–[3]. The success further provokes the flourish of customized neural network accelerators with massive parallel processing engines which typically offer much higher performance and energy efficiency compared to general purposed processors (GPPs) [4]–[8]. While the performance of neural network accelerators has been intensively optimized from various angles like pruning and quantization, the reliability of the accelerators especially the ones that are deployed on FPGAs remains not well-explored.

The shrinking semiconductor technology greatly improves the transistor density of chips, but the circuits with smaller feature size are more susceptible to manufacturing defects and abnormal physical processes like thermal stress, electromigration, hot carrier injection, and gate oxide wear-out. Thereby, the persistent (hard) faults become one of the major sources of system unreliability. Despite the fault-tolerance of neural network models, permanent faults in neural network accelerators can cause computing errors and considerable wrong predictions [9]. They may even lead to disastrous consequences to some of the mission-critical applications such as self-driving, nuclear power plants, and medical diagnosis, which are sensitive to neural network prediction mistakes.

It is seminal to comprehend the impact of errors on neural network accelerators to improve the model functioning. To this end, several research works are published that contain

methods to identify errors in neural network accelerators [10]–[14]. However, they usually experimented with simulators and focused on the influence of hardware faults on the prediction accuracy of the neural network models. For instance, the authors in [10] mainly investigated the data faults of weights, activities, and hidden states, which are stored in on-chip buffers. Then they explored the neural network model resilience with model-wise analysis and layer-wise analysis. The work in [13] targeted at the analysis of software errors in DNN accelerators and explored the error propagation behaviors based on the structure of the neural networks, data types and so on.

The simulation based approaches are fast and flexible for analyzing neural network computing and prediction accuracy, but they typically ignore critical controlling details and interfaces of the DNN accelerators to ensure the simulation speed. Nevertheless, hardware faults on these components may have considerable influence to the overall acceleration system other than the prediction accuracy loss. For instance, faults in DMA module may result in illegal memory accesses and corrupt the system. This must be addressed to guarantee reliable DNN acceleration especially in mission-critical applications. In addition, many DNN accelerators are implemented on FPGAs for more intensive customization and convenient reconfiguration. While the functionality of the DNN accelerators is mapped to the FPGA infrastructures instead of the primitive logic gates, the simulation based approaches that usually inject errors to the operations used in DNN processing do not apply to the FPGA based DNN acceleration system. Because hardware faults in FPGAs affect the configuration of the devices instead of the accelerator components directly while the actual parts of the accelerators that are influenced depends on the FPGA placing and routing.

To gain further insight of faults in DNN accelerators, we conduct the fault analysis on running ARM-FPGA system where FPGA has a representative DNN accelerator with 2D systolic array implemented along with hardware fault injection modules and shares the DRAM with the ARM processors. Since the fault distribution models are implemented with software on the ARM processors, they are convenient to change for fault analysis using different models. Aside from that we work with four different models for detecting the others.

Li, Shunlong et. al. [15] operated one-dimensional convolutional neural network along the time axis to capture the

temporal dependency. Shi, Chong et. al [16]’s work focuses on the internal leakage fault diagnosis caused by the wear based on intrinsic mode functions (IMFs). Unlike prior works that focused on prediction accuracy loss analysis, we try to analyze the behaviours of the DNN accelerators under hardware faults and investigate the system functionality, fault coverage, input variation. Particularly, we study the system stall that dramatically destroys the system functionality in detail and present a simple yet efficient approach to alleviate the problem.

The following lines sum up our contributions to the literature:

- Our system focuses on fault analysis of neural network accelerators on ARM-FPGAs. To make the analysis easier, it provides high-level interfaces for both fault injection and output data comparison of neural network models.
- On top of the fault analysis system, we mainly classify and analyze the resulting behaviors of the DNN accelerators from system point of view. On top of the prediction accuracy, we also study the fault coverage, system functionality, input variation when the accelerators are exposed to persistent faults.
- With comprehensive experiments over representative models, we observe that system stalls that can destroy the system functionality of DNN accelerators cannot be ignored. And we further show that errors in data movement instructions is a key reason for the system stalls, which can be addressed with negligible hardware overhead.

The remainder of the paper can be described in the following paragraphs. Section II sheds light on, the introduction to deep learning neural networks and a typical DNN accelerators with 2D computing array. In Section III, we describe the proposed framework on ARM-FPGAs and elaborate on the major aspects that we will investigate from system point of view. Section IV details the results and evaluation. In Section V, we give a brief review of prior fault tolerant analysis and design of neural network accelerators. Finally, we conclude this work in Section VI.

II. BACKGROUND

The main causes of unreliability are hardware flaws in DNN accelerators. The impact of errors is inextricably linked to the microarchitecture of the DNN accelerators. In this part, we take a standard DNN accelerator with a normal 2D processing element (PE) array as an example and develop its design to assist understand and study the fault tolerance of the accelerators.

Figure 1 depicts a sample DNN accelerator. It uses output stationary data flow to transfer computations like convolution to a 2D computing array. Every PE completes all of the processes necessary to produce an output activation. While each PE just has a single multiplier and accumulator, it progressively accumulates all input activations in a filter window. While input activations are organized in a batch and sent to

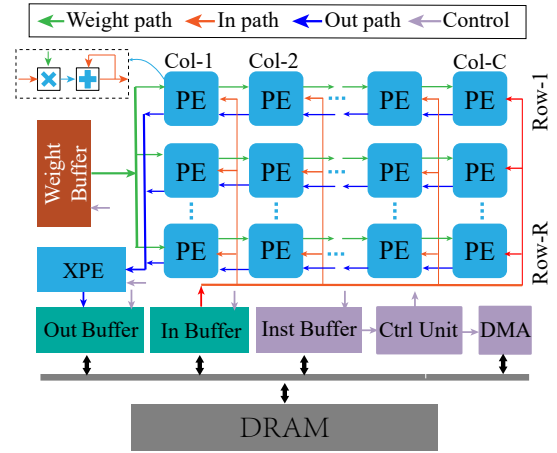


Fig. 1. Typical DNN accelerator architecture

one column of PE every cycle, each PE in the column shares the same input data through broadcasting and it takes each PE multiple cycles to complete the accumulation. During this period, more batched input activations can be read and sent to the next column of PEs along with the movement of the weights. Output activations flow from right to left in column-wise. Eventually, each row of the PEs array produces a set of sequential output activations in the same row of one output feature map on y-axis. The architecture along with the compact data flow achieves high data reuse under limited on-chip buffer bandwidth provision.

Both convolution layer and full connection layer can be mapped to the array efficiently. While pooling and other non-linear activation functions such as sigmoid will be performed right after the computing-intensive layers like convolution layer in a module named XPE such that the data movement between the two layers can be reduced. All the neural network operations can be mapped to the accelerator. To associate the models with various layer combinations and characteristics such as stride size and kernel size, we define a set of instructions to generate appropriate control signals for different neural network operations. Each neural network will be compiled to a series of instructions and executed sequentially. In addition, neural network input features and weights are usually larger than the on-chip buffers and PE array size, so they must be tiled and the tiles need to be scheduled to obtain efficient execution on the accelerator. To enable fine-grained optimizations, each instruction only handles operations of a single tile. Thus, tiling is performed during model compilation and it is transparent to the instructions.

Table I shows the instruction set of the neural network accelerator. It adopts 64-bit fixed length encoding and consists of four types of instructions including parameter setup, calculation, data movement and control. The parameter setup category defines the input/output feature size, kernel size, Q-code, and DMA parameter. Calculation category includes different operations in neural networks such as convolution, full connection, pooling, addition, softmax, dot-accumulation

TABLE I
INSTRUCTION SET OF THE DNN ACCELERATOR

Instruction Type	Description
Parameter setup	Setup parameters for the computing operations such as the input/output feature size, kernel size, Q-code, and DMA options
Calculation	Performs various neural network operations such as convolution, full connection, pooling, addition, softmax, dot-accumulation and activation function
Data movement	Move a block of data from buffer to buffer, buffer to DRAM and DRAM to buffer.
Control	Control the execution of the accelerator such as Jump, Nop and Stop

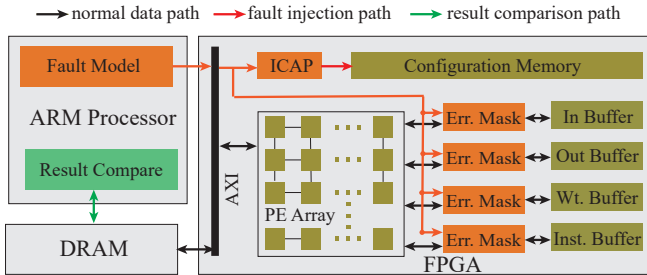


Fig. 2. Overview of the fault analysis system

and activation function etc. Data movement category includes three instructions which move a block of data from DRAM to buffer, buffer to DRAM and buffer to buffer respectively. Finally, control category includes three instructions which are Jump, Stop and Nop. Jump instruction is mainly used for repeated execution. Stop is used to terminate the execution of the accelerator. Nop is used to resolve the data dependency between sequential instructions.

The neural network accelerator architecture is general enough to support various neural network models. In addition, it typically works along with a general purposed processor and has an AXI slave port that allows configuration and controlling from the attached processor. It assumes the input data, weight and output data are stored in DRAM that can be accessed directly.

III. DNN ACCELERATION FAULT ANALYSIS PLATFORM AND FAULT CLASSIFICATION

A. Fault Analysis Platform

We built a fault analysis platform as represented in Figure 2. It has an unusual neural network accelerator based on FPGA.

In addition to this system, we needed a module as present in Figure 2. The fault injection data path is marked with orange arrows. It is implemented on both the ARM processor and FPGA. The FPGA errors are prevalent in the four different memory types.

For FPGA configuration memory, we leverage Xilinx ICAP port [17], that allows user logic to access configuration memory, to inject errors. We select the frames and the number of bits for each bit error injection arbitrarily. It is possible that the

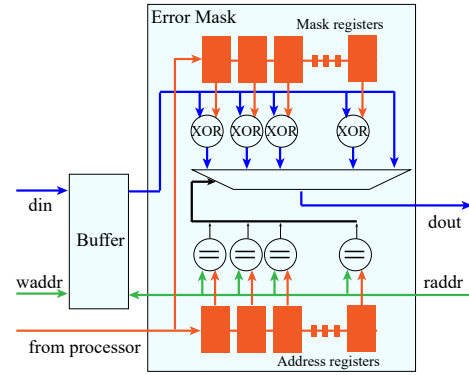


Fig. 3. Error mask for fault injection to on-chip memory

error may be present at any location of the FPGA configuration memory. After finding the error location, we read the whole frame out of the configuration memory [18], change the victim bit in the frame, and write it back to the configuration memory [19].

We also produce an injection mask for block RAM and distributed memory as represented in Figure 3. It essentially consists of a collection of address and mask registers. The addresses in the registers reflect the positions of the faults to be injected, while the associated masks keep track of the precise error bits.

Another important part of the fault analysis platform is the result collection and comparison. We have the output of neural networks stored in the shared DRAM, which can be easily accessed on the ARM processor and compared to the pre-calculated golden reference. In addition, the computing results produced in the intermediate layers can also be compared. The result comparison is mainly performed on the ARM processor and can be easily utilized for further analysis by high-level application designers.

B. System fault classification

Prior fault analysis works usually focus on computing errors of the neural networks and the incurred prediction accuracy loss. We argue that the consequences of hardware faults on a DNN acceleration system vary and should be classified into more categories. Table II shows the proposed classification. From the perspective of a system, the consequences caused by hardware faults roughly include system exception and accuracy degradation. System exception indicates that the neural network execution behaves abnormally, which may be stalled without returning or returns too fast or too slow. Basically, we define them as system stall and abnormal runtime. For the accuracy degradation, we further classified into two cases including system stall and abnormal runtime.

We chose Neural Networks in four different application scenarios and try to analyze the differences of error tolerance in different application scenarios and networks. The four network applications include ResNet network for image classification, YOLO system for target detection, LSTM network for voice classification, and DCGAN network for image generation. We

TABLE II
HARDWARE FAULTS

system exception	system stall
	abnormal runtime
Accuracy degradation	L_0
	...
	L_k

will evaluate their fault tolerance from accuracy and output consistency.

Neural Network accelerators injected with hardware errors may produce unexpected conditions. We define the system halt situation, which refers to a serious error in the system, or working improperly. such as unable to read and write registers, timeout, abnormal short runtime, etc. When the system halts, we need to reset the FPGA and restart the system. System halt situations are considered the result of errors in the evaluation of network accuracy and are listed separately in the output consistency.

Network accuracy refers to the overall accuracy of the network when performing corresponding tasks, such as the accuracy of 20,000 image recognition. When there are errors in the operation, the accuracy of the network will show a downward trend. For classification networks including ResNet and LSTM, top-5 accuracy is used to evaluate their accuracy, and for the YOLO system, mAP is adopted.

Output consistency is the difference between the result of running with errors injected and the result of normal running. We ran the corresponding data set when no errors are injected into each network at first, and defined the results as standard output. The results of Neural Networks prediction injected with errors are divided into two categories: result with deviation and result match. Result with deviation refers to system works properly with output differently from standard output. Result match means that the system works properly and the outputs are still standard output.

For the result with deviation case, we define its deviation quantitatively and further subdivide the result. Due to the different application functions of each network, the evaluation criteria of deviation are also different. For YOLO system, the result is the target detection bounding box, and when the detection result does not match the standard output in object type, it is defined as detection result error. When the result target type is consistent, the error is defined as the intersection area of the error output and the standard output divided by the area of the union. Target types not match for one single level, the two do not overlap with each other for one level, and then each 20% is divided into one level. For ResNet and LSTM, the outputs are top-5 labels. When the error output is not completely consistent with the standard output, the number of elements in the intersection of the two is taken, and divide the levels refer to the number. For DCGAN, we used the universal SSIM standard, and divided it into six levels according to the actual visual effects: 0 10%, almost impossible to recognize; 10 20%, barely visible; 20 50%, with large deformation or distortion; 50 80% with partial deformation or distortion;

TABLE III
UTILIZATION REPORT OF FAULT ANALYSIS PLATFORM

Resource	Utilization	Available	Utilization Percentage
LUT	122618	218600	56.09%
LUTRAM	185	70400	0.26%
FF	84641	437200	19.36%
BRAM	203	545	37.25%
DSP	297	900	33%
MMCM	1	8	12.5%

80 90%, small deformation or distortion can be seen; 90 100%, almost no deformation or distortion is visible.

IV. EXPERIMENT

We seek to understand the influence of persistent errors on FPGA-based neural network acceleration system. Particularly, we try to analyze the influence from a system point of view and figure out the underlying reasons for severe system problems such as system stall and dramatic prediction accuracy loss.

A. Device and Environment

Xilinx Zynq-7000 SoC ZC706 Evaluation Board will be used in the experiments' hardware implementation. It has appropriate hardware resources and is easy to develop and use. The hardware design and Bitstream file compilation were completed using the upper computer with Intel Core i7-6700 processor and 2x8GB DDR4 2400MHz memory. The system environment used was Ubuntu 16.04 LTS version, and Xilinx Vivado Design Suite and Xilinx Software Development Kits version 2017.4.

The hardware resource utilization of the error analysis platform implementation on ZC706 is shown in Table III.

The four models cover a broad range of applications. Yolo represent a typical neural network model for object detection [20], Resnet is a widely adopted neural network model for classification [21], LSTM is the mostly used neural network model for audio classification tasks [22], and DCGAN stands for a typical neural network model for generative tasks [23].

Despite the widespread adoption of deep learning neural network on various applications, it is particularly successful in four categories of tasks including object detection, object classification, voice recognition and style transfer. Among a great number of neural network models, Yolo, Resnet, LSTM and DCGAN are four typical neural networks that are comprehensively explored to handle the four computing tasks respectively.

B. Overview

We hope to explore the possible consequences of errors, the fault-tolerant ability of different applications and the influence of different error locations of accelerators, which can provide meaningful references for the subsequent network optimization and the fault-tolerant design of accelerators.

We conducted five sets of experiments, which explained the influence of single error on different networks, the difference of fault tolerance ability of different applications, the error

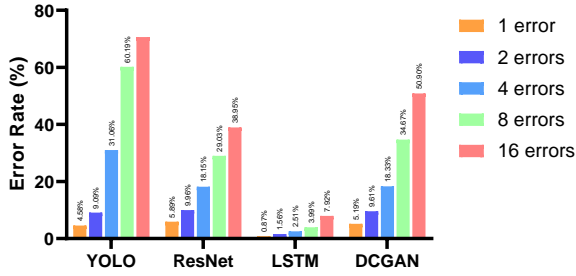


Fig. 4. Application error rate caused by single-bit random hardware error

classification of different applications, the influence of different accelerator units and whether the input data affected the error representation.

C. Error Consequences and Coverage

First, we conducted single-bit random error injection experiments for different applications, and conducted 20,000 runs for each application, to analyze the proportion of single-bit random error shielded in the system and the possible influence of single-bit random error on the accelerator system. Figure 4 shows the percentage of application errors caused by a single-bit random hardware error. In the experiment, we found that more than 90% of the errors were masked by software or hardware. However, while most errors are masked without impact to the operation, a single-bit error can lead to serious exceptions, including system halt, serious deviation in results, and so on. In addition, LSTM network has a better fault tolerance performance than other three networks, and the proportion of the influence caused by single error of the other three networks is about 5-7 times that of LSTM. According to our analysis, this is because LSTM network is smaller than other networks and uses less storage and computing resources.

D. Effect of Error Number

We completed a single run with errors injected number of powers of 2, with 20,000 runs for each network. In general, the proportion of system halt and result with deviation increases with the number of errors, and the accuracy of application decreases. Figure 6 shows the proportion of system halt and result deviation, and Figure 5 shows the accuracy of each network. We found that the influence of multiple errors on the accelerator was obvious and far beyond our expectation. The Neural Network accelerator is still vulnerable to errors. By the time we injected 16 errors in a single run, the system halt rate was more than 1%, means it took more time to restore the system than to run it. From the perspective of network accuracy, take YOLO system as an example, its mAP decreases by 8.95% when it runs with 16 errors, means the application function of the system is also seriously affected.

The result with deviation proportion of different networks appears differently with the increase of error number. When 16 errors are injected, LSTM network still has a small result deviation proportion due to its small network structure. The

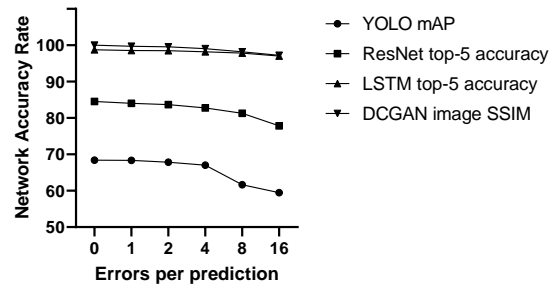
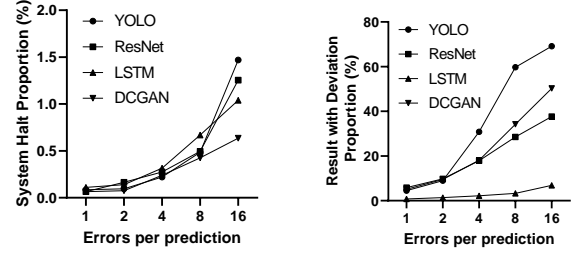


Fig. 5. Network accuracy versus error number



(a) System halt

(b) Result with deviation

Fig. 6. Abnormal situation proportion versus error number

proportion of YOLO system is very high, with about 70% of the results showing errors. ResNet is relatively low, with only about 35% result deviation. DCGAN network is in between, and about 50% of the results have numerical errors. We believe that the result deviation may be related to the structure of the output. The output of YOLO system contains more information such as object type, location and size of bounding box, etc., and the output of ResNet is simple sorting, while the simple output is obviously less susceptible to errors.

E. Details of Result with Deviation

The results with errors are further classified and analyzed. In general, most of the errors are small, with a certain proportion of serious errors and relatively few moderate ones. We believe that most of the errors do not belong to the errors with global influence, but only affect one or several calculations. For example, a single value in the convolution kernel changes. Alternatively, a portion of the error is masked by subsequent calculations such as the max pooling layer. Some errors may have an impact on the control path or the reusable module, resulting in the accumulation of errors throughout the calculation; Or errors that cause serious deviations in the data, such as sign bit upset, can have serious consequences. Figure 7 shows the details of result distribution of result with deviation situations.

Specific to each network, about 70% of the YOLO system's errors belong to the level of bounding box overlap ratio more than 80%. The total of object type errors and non-overlapping boxes is about 20%. The remaining 10% or so is moderate errors. We think this is caused by the implementation of YOLO. YOLO divides the input images into a series of grid

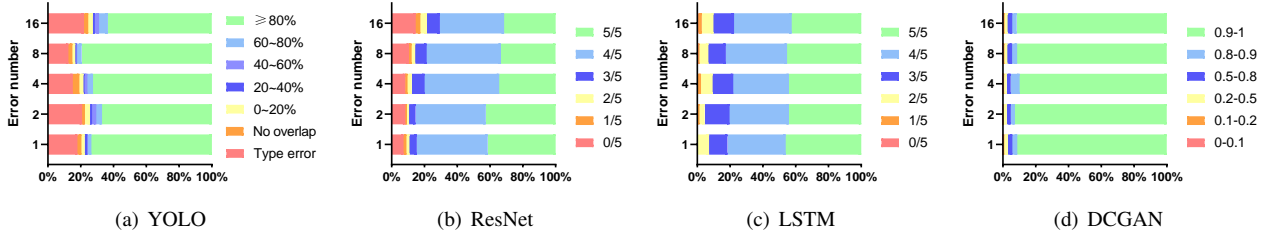


Fig. 7. Distribution of result with deviation situations

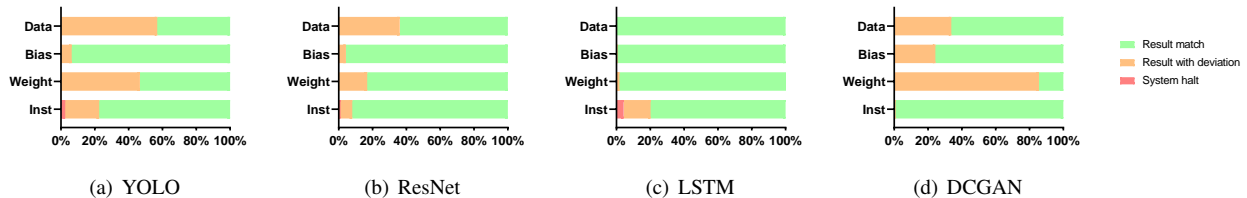


Fig. 8. Proportion of different error location

cells, and each grid cell is only responsible for one kind of object. Moreover, there is a binary judgment $\text{Pr}(\text{Object})$ whether there is a target or not in the confidence degree, which leads to more object type error cases. The bounding boxes that are given after object recognition based on relative wide and high are less sensitive.

More than 70% of the errors in the ResNet and LSTM classification networks were small impact results of matching four or five items. We think this is because the output is SoftMax layer, which is less affected by the error, and the error is easy to be hidden when sorting, so the result only shows a small alter. However, with the increase of the number of errors, the proportion of serious errors of no matching item in ResNet results increased with the increase of the number of errors and exceeded 10%. Serious errors cannot be hidden, and the networks fault tolerance for multiple errors is relatively limited.

The result of DCGAN is about 90% of the results are small deviation level of more than 90% of SSIM. Only a few of them have a large deviation. Combined with the image, in 90% of the small deviation results compared with the standard output, basically no difference can be directly seen, and only a few large deviation results have serious distortion of the image. Considering that the output is picture information, these small deviations can be ignored without affecting the visual effect, we believe that DCGAN has relatively strong error tolerance.

F. Effect of Error Location

In this period, we conducted the experiment results of different error locations. We injected a single-bit random error into a designated location, and conducted multiple experiments to observe the performance of the network. By analyzing the influence of error in different locations on the accelerator, it can provide specific methods for the subsequent fault-tolerant design.

TABLE IV
INSTRUCTION CHANGE

Situation	Percentage
Error instruction undefined	2.48%
Instruction type change	7.45%
Abnormal parameter	90.06%

In general, the system is less affected by configuration memory errors, considering that the error injection of configuration memory is global, whose errors may not affect the system. Errors in configuration memory can cause system halt or result with deviation. Errors in BRAMs used for instruction buffer can cause system halt or result with deviation, while BRAMs used in other type buffers can only cause numerical deviations.

We focus on the analysis of the system halt situations caused by error in instruction buffer, which take about 20% part of the system halt situations. Compared with the instruction before and after upset, the system halts caused by instruction errors includes three situations: instruction type changes, wrong instruction not defined, and the parameter in the operation is abnormal. Different instruction types of the original instruction are considered. Table IV and Table V shows the detail of instruction error. About 50% of the system halt situations are caused by the error of DMA instructions. The abnormal access address or boundary violation caused by the abnormal parameters of DMA instruction will lead to the system halt. About 30% are caused by AGU instruction errors, which result in abnormal in-chip control flow.

The proportions of errors in instruction buffer led to system halt in ResNet, YOLO and LSTM, reached 1.15%, 2.55% and 4.25% respectively, seriously affecting the proper application of the system. For result with deviation case, in the experiment of YOLO, about half of the result deviation situations caused by instruction buffer errors were serious object type errors. In the experiment of ResNet, a large number of mismatches

TABLE V
ORIGINAL INSTRUCTION TYPE

type	Percentage
DMA	55.90%
AGU	32.92%
others	11.18%

were also caused. DCGAN network is limited by instruction errors, because the instruction sequence length of this network is very short, only 2% of the instruction buffer is used, while the instruction sequence of other networks uses instruction buffer of 50%~80%. Combined with the result with deviation and system halt case, we propose that instruction buffer needs to be strengthened in the fault-tolerant design.

Errors in the buffers used in data-flow, such as weights, data, and bias buffer, do not cause system halt, only may cause result deviations. In general, data and weights are more sensitive than bias. Taking YOLO system as an example, the proportion of result deviation caused by single error in weight, data and bias buffer is 48.75%, 56.95% and 6.35% respectively. Horizontal comparison shows that each network has different sensitivity to different buffer errors, as shown in figure .

G. Input-Related Error

In the above experiments, we used different input data for experiments, and we verified the relationship between errors and input data in this set of experiments. We test different input data using the same error. Whether a hardware error causes an application error exists in two ways, depending on the input data or not. Errors unrelated to input data, fixed to cause system halt or result deviation, or be masked, that is, different input data will not influence the classification of the result. The other part of the errors is input data related, which can be shown as replacing different input data, result match situation and result with deviation situation both appear. In other words, different input data has different sensitivity to an input-related error. We believe that this is caused by structures which error affected. Input-unrelated errors may affect the control-flow of the system, the bus, etc. These structures are used in every operation, and the errors will not be masked by subsequent calculations. Input-related errors may affect the relevant data in the data-flow, and some errors may be masked in the subsequent calculation. Due to the large number of experiments, we only observed this phenomenon without further study on its proportion and distribution.

V. RELATED WORK

Deep learning accelerators that ensure both high performance and energy efficiency of neural network are increasingly adopted in various computing devices including IoT devices, mobile phones and cloud. While the accelerators fabricated with the latest semiconductor technology is susceptible to the manufacturing defects and abnormal processes due to the small transistor feature size, the number of hardware faults grows accordingly. The faults may further lead to computing errors, dramatic prediction accuracy loss and even system stall

when the faults are not handled appropriately. For some of the mission-critical applications, the prediction mistakes may even cause catastrophic failures.

To gain insight of fault tolerance of neural network accelerators, the authors in [13] investigated the influence of data types, values, data reuses, and types of layers on the resilience of DNN accelerators through experiments on a DNN simulator. error resilience of xxx with simulation. Different from xxx, the works in xxx mainly focus on the difference of fault tolerance using different data types. Some of the researchers try The reliability of the neural network accelerators While neural networks with large amount of redundant computing is considered to resilient, Reliability of neural network accelerators become critical to resilient neural network execution. 1) Reliability espeically FPGA based reliability problem 2) The prevalence of deep learning neural networks provokes the development of convolutional neural network (CNN) accelerators for both higher performance and energy efficiency. existing fault-tolerant CNN accelerator works,

Data type analysis with simulation, error propagation analysis Retraining to improve fault tolerance and tolerate the computing errors (Change the neural network model) Computing array based fault model Relax the design constraints and have the accelerator obtain advantageous design trade-off between precision and performance.DAC'18 work Basically, the analysis focuses on the computing of the neural network. Hardware structure is not discussed in detail. Simulation is the major approach. lack of system analysis on a CPU-CNN accelerator. FPGA based analysis is not covered. Prior FPGA based reliability such as soft processors etc. It is not quite relevant. Neural network inherent fault tolerance. Error analysis on a running system remains not explored.

FPGA is a widely used hardware platform, and there are many designs and methods for error injection on FPGAs [24] [25] [26] [27]. FPGA-based (also known as emulation-based) error analysis is widely used in soft processor sensitivity analysis and other scenarios. The FPGA-based fault injection techniques have good controllability, observability and ideal speed.

FPGA-based fault injection techniques can be divided into two categories: reconfiguration-based techniques and instrument-based techniques. The reconfiguration-based techniques rely on the internal mechanism of FPGAs. These techniques use complete or partial reconfiguration to change the configuration bit of the FPGA device to apply the target fault model to the desired fault location. The reconfiguration process is a speed bottleneck for reconfiguration-based techniques. In instrument-based technology, fault injection modules called saboteur are added to each fault point, and fault is injected by activating the saboteurs. Instrument-based techniques have higher speed than reconfiguration-based techniques, while implementing the saboteurs increase the area of the circuit. We shall design the saboteurs ourselves for instrument-based techniques, and insert them into the design under test.

VI. CONCLUSION

With the wide application of neural network in many scenarios with high safety requirements like autonomous driving, the fault-tolerant performance of neural network accelerators has received more attention. In this paper, we designed a fault emulation and analysis system for neural network accelerator based on SRAM-based FPGA, and completed a series of experiments on this basis. We find that the fault tolerance of neural network accelerator is poor, and analyze the misrepresentation of different numbers, different network applications and different error locations. These analyses provide a reference for the following fault-tolerant design.

REFERENCES

- [1] L. A. Gatys, A. S. Ecker, and M. Bethge, "Image style transfer using convolutional neural networks," in *The IEEE Conference on Computer Vision and Pattern Recognition (CVPR)*, June 2016.
- [2] R. Collobert and J. Weston, "A unified architecture for natural language processing: Deep neural networks with multitask learning," in *Proceedings of the 25th International Conference on Machine Learning*, ser. ICML '08. New York, NY, USA: ACM, 2008, pp. 160–167. [Online]. Available: <http://doi.acm.org/10.1145/1390156.1390177>
- [3] C. Chen, A. Seff, A. Kornhauer, and J. Xiao, "Deepdriving: Learning affordance for direct perception in autonomous driving," in *The IEEE International Conference on Computer Vision (ICCV)*, December 2015.
- [4] T. Chen, Z. Du, N. Sun, J. Wang, C. Wu, Y. Chen, and O. Temam, "Dianna: A small-footprint high-throughput accelerator for ubiquitous machine-learning," in *ACM Sigplan Notices*, vol. 49, no. 4. ACM, 2014, pp. 269–284.
- [5] Y. Chen, T. Luo, S. Liu, S. Zhang, L. He, J. Wang, L. Li, T. Chen, Z. Xu, N. Sun *et al.*, "Dadianna: A machine-learning supercomputer," in *Proceedings of the 47th Annual IEEE/ACM International Symposium on Microarchitecture*. IEEE Computer Society, 2014, pp. 609–622.
- [6] Y.-H. Chen, J. Emer, and V. Sze, "Eyeriss: A spatial architecture for energy-efficient dataflow for convolutional neural networks," in *ACM SIGARCH Computer Architecture News*, vol. 44, no. 3. IEEE Press, 2014, pp. 367–379.
- [7] C. Zhang, P. Li, G. Sun, Y. Guan, B. Xiao, and J. Cong, "Optimizing fpga-based accelerator design for deep convolutional neural networks," in *Proceedings of the 2015 ACM/SIGDA International Symposium on Field-Programmable Gate Arrays*, ser. FPGA '15. New York, NY, USA: ACM, 2015, pp. 161–170. [Online]. Available: <http://doi.acm.org/10.1145/2684746.2689060>
- [8] S. Han, X. Liu, H. Mao, J. Pu, A. Pedram, M. A. Horowitz, and W. J. Dally, "Eie: Efficient inference engine on compressed deep neural network," in *2016 ACM/IEEE 43rd Annual International Symposium on Computer Architecture (ISCA)*, June 2016, pp. 243–254.
- [9] P. W. Protzel, D. L. Palumbo, and M. K. Arras, "Performance and fault-tolerance of neural networks for optimization," *IEEE Transactions on Neural Networks*, vol. 4, no. 4, pp. 600–614, July 1993.
- [10] B. Reagen, U. Gupta, L. Pentecost, P. Whatmough, S. K. Lee, N. Mulholland, D. Brooks, and G.-Y. Wei, "Ares: A framework for quantifying the resilience of deep neural networks," pp. 1–6, 2018.
- [11] F. Kausar and P. Aishwarya, "Artificial neural network: Framework for fault tolerance and future," in *2016 International Conference on Electrical, Electronics, and Optimization Techniques (ICEEOT)*, March 2016, pp. 648–651.
- [12] G. Li, K. Pattabiraman, and N. Debardeleben, "Tensorfi: A configurable fault injector for tensorflow applications," in *2018 IEEE International Symposium on Software Reliability Engineering Workshops (ISSREW)*, 2018.
- [13] G. Li, S. K. S. Hari, M. Sullivan, T. Tsai, K. Pattabiraman, J. Emer, and S. W. Keckler, "Understanding error propagation in deep learning neural network (DNN) accelerators and applications," pp. 1–12, 2017.
- [14] B. Salami, O. Unsal, and A. Cristal, "On the Resilience of RTL NN Accelerators: Fault Characterization and Mitigation," 2018. [Online]. Available: <http://arxiv.org/abs/1806.09679>
- [15] S. Li, J. Niu, and Z. Li, "Novelty detection of cable-stayed bridges based on cable force correlation exploration using spatiotemporal graph convolutional networks," *Structural Health Monitoring*, p. 1475921720988666, 2021.
- [16] C. Shi, Y. Ren, H. Tang, and L. R. Mupfukirei, "A fault diagnosis method for an electro-hydraulic directional valve based on intrinsic mode functions and weighted densely connected convolutional networks," *Measurement Science and Technology*, vol. 32, no. 8, p. 084015, 2021.
- [17] Xilinx Inc., "Vivado design suite 7 series fpga and zynq-7000 soc libraries guide," http://www.xilinx.com/support/documentation/sw_manuals/xilinx2017_4/ug953-vivado-7series-libraries.pdf, Dec 2018, UG953(v2017.4).
- [18] —, "Axi hwicap v3.0 logicore ip product guide," http://www.xilinx.com/support/documentation/ip_documentation/axi_hwicap/v3_0/pg134-axi-hwicap.pdf, Oct 2016, PG134.
- [19] —, "7 series fpgas configuration user guide," http://www.xilinx.com/support/documentation/user_guides/ug470_7Series_Config.pdf, Aug 2018, UG470 (v1.13.1).
- [20] J. Redmon and A. Farhadi, "Yolo9000: Better, faster, stronger," *arXiv preprint arXiv:1612.08242*, 2016.
- [21] K. He, X. Zhang, S. Ren, and J. Sun, "Deep residual learning for image recognition," in *The IEEE Conference on Computer Vision and Pattern Recognition (CVPR)*, June 2016.
- [22] H. Sak, A. Senior, and F. Beaufays, "Long short-term memory recurrent neural network architectures for large scale acoustic modeling," in *Fifteenth annual conference of the international speech communication association*, 2014.
- [23] A. Radford, L. Metz, and S. Chintala, "Unsupervised representation learning with deep convolutional generative adversarial networks," *arXiv preprint arXiv:1511.06434*, 2015.
- [24] M. Ebrahimi, A. Mohammadi, A. Ejlali, and S. G. Miremadi, "A fast, flexible, and easy-to-develop fpga-based fault injection technique," *Microelectronics Reliability*, vol. 54, no. 5, pp. 1000–1008, 2014.
- [25] C. Lopez-Ongil, L. Entrena, M. Garcia-Valderas, M. Portela, and F. Munoz, "A unified environment for fault injection at any design level based on emulation," *IEEE Transactions on Nuclear Science*, vol. 54, no. 4, pp. 946–950, 2007.
- [26] N. A. Harward, M. R. Gardiner, L. W. Hsiao, and M. J. Wirthlin, "Estimating soft processor soft error sensitivity through fault injection," in *IEEE International Symposium on Field-programmable Custom Computing Machines*, 2015.
- [27] J. Tarrillo, J. Tonfat, L. Tambara, F. L. Kastensmidt, and R. Reis, "Multiple fault injection platform for sram-based fpga based on ground-level radiation experiments," in *Test Symposium*, 2015.